

# Thermodynamic properties of tellurite ( $\beta$ -TeO<sub>2</sub>), paratellurite ( $\alpha$ -TeO<sub>2</sub>), TeO<sub>2</sub> glass, and Te(IV) phases with stoichiometry $M_2Te_3O_8$ , $MTe_6O_{13}$ , $MTe_2O_5$ ( $M^{2+} = Co, Cu, Mg, Mn, Ni, Zn$ )

Juraj Majzlan<sup>a,\*</sup>, Stefanie Notz<sup>a</sup>, Patrick Haase<sup>a</sup>, Efstratios I. Kamitsos<sup>b</sup>, Nagia S. Tagiara<sup>b</sup>, Edgar Dachs<sup>c</sup>

<sup>a</sup> Institute of Geosciences, Friedrich-Schiller University, Burgweg 11, 07749 Jena, Germany

<sup>b</sup> Theoretical and Physical Chemistry Institute, National Hellenic Research Foundation, 48 Vass Constantinou Ave., 11635 Athens, Greece

<sup>c</sup> Department of Chemistry and Physics of Materials, University of Salzburg, Jakob-Haringer-Strasse 2a, 5020 Salzburg, Austria

## ARTICLE INFO

Handling Editor: Astrid Holzheid

### Keywords:

Tellurium oxides  
Tellurites  
Thermodynamics

## ABSTRACT

Thermodynamic properties of several TeO<sub>2</sub> polymorphs and metal tellurites were measured by a combination of calorimetric techniques. The most stable TeO<sub>2</sub> polymorph is  $\alpha$ -TeO<sub>2</sub>, with its enthalpy of formation ( $\Delta_f H^\circ$ ) selected from literature data as  $-322.0 \pm 1.3 \text{ kJ}\cdot\text{mol}^{-1}$ .  $\beta$ -TeO<sub>2</sub> is metastable (in enthalpy) with respect to  $\alpha$ -TeO<sub>2</sub> by  $+1.40 \pm 0.07 \text{ kJ}\cdot\text{mol}^{-1}$ , TeO<sub>2</sub> glass by a larger amount of  $+14.09 \pm 0.11 \text{ kJ}\cdot\text{mol}^{-1}$ . >200 experimental runs and post-synthesis treatments were performed in order to produce phase-pure samples of Co, Cu, Mg, Mn, Ni, Zn tellurites. The results of the hydrothermal and solid-state syntheses are described in detail and the products were characterized by powder X-ray diffraction. The standard thermodynamic data for the Te(IV) phases are (standard enthalpy of formation from the elements,  $\Delta_f H^\circ$  in  $\text{kJ}\cdot\text{mol}^{-1}$ , standard third-law entropy  $S^\circ$  in  $\text{J}\cdot\text{mol}^{-1}\cdot\text{K}^{-1}$ ): Co<sub>2</sub>Te<sub>3</sub>O<sub>8</sub>:  $\Delta_f H^\circ = -1514.2 \pm 6.0$ ,  $S^\circ = 319.2 \pm 2.2$ ; CoTe<sub>6</sub>O<sub>13</sub>:  $\Delta_f H^\circ = -2212.5 \pm 8.1$ ,  $S^\circ = 471.7 \pm 3.3$ ; MgTe<sub>6</sub>O<sub>13</sub>:  $\Delta_f H^\circ = -2525.8 \pm 7.9$ ,  $S^\circ = 509.2 \pm 3.6$ ; Ni<sub>2</sub>Te<sub>3</sub>O<sub>8</sub>:  $\Delta_f H^\circ$  not measured,  $S^\circ = 293.3 \pm 2.1$ ; NiTe<sub>6</sub>O<sub>13</sub>:  $\Delta_f H^\circ = -2198.7 \pm 8.2$ ,  $S^\circ = 466.5$  (estimated); CuTe<sub>2</sub>O<sub>5</sub>:  $\Delta_f H^\circ = -820.2 \pm 3.3$ ,  $S^\circ = 187.2 \pm 1.3$ ; Zn<sub>2</sub>Te<sub>3</sub>O<sub>8</sub>:  $\Delta_f H^\circ = -1722.5 \pm 4.0$ ,  $S^\circ = 299.3 \pm 2.1$ . The solubility calculations show that the Te(IV) concentration in an aqueous phase, needed to produce such phases, must be at least 3–5 orders of magnitude higher than the natural Te background concentrations. The occurrence of these minerals, as expected, are restricted to hotspots of Te concentrations. In order to produce more reliable phase diagrams, more work needs to be done on the thermodynamics of potential competing phases in these systems, including Te(VI) phases.

## 1. Introduction

Tellurium is a rare but a mineralogically exceptionally diverse element (Christy, 2015). Given its crustal abundance of only 0.001 ppm (reported by Christy, 2015), it is an essential element in >190 minerals. Note that the precise value of Te crustal abundance is still a matter of debate (see Filella et al., 2019). Tellurium is found in primary minerals, mostly in the oxidation state –II, such as hessite (Ag<sub>2</sub>Te), altaite (PbTe), or coloradoite (HgTe). In secondary minerals, the common oxidation states are +IV and +VI.

Tellurium(IV) oxide, TeO<sub>2</sub>, is polymorphic and known from nature as the minerals tellurite ( $\beta$ -TeO<sub>2</sub>, space group *Pbca*) and paratellurite ( $\alpha$ -TeO<sub>2</sub>, space group *P4<sub>1</sub>21*). A synthetic  $\gamma$ -TeO<sub>2</sub> polymorph can be

obtained by devitrification of TeO<sub>2</sub> glass (Blanchandin et al., 1999; Li et al., 2010; Weil, 2017). In addition, pure TeO<sub>2</sub> glass and glasses based on TeO<sub>2</sub> were investigated in great detail because of a number of promising physical properties (Tagiara et al., 2017).

Metal tellurites include phases with the stoichiometry  $M_2Te_3O_8$ ,  $MTe_6O_{13}$ , and  $MTe_2O_5$ . They were targeted in this work because some of them are known as minerals. Most of the phases with this stoichiometry were prepared previously in the laboratory (Table 1), only a few of them are unknown so far.

The phases with the stoichiometry  $M_2Te_3O_8$  are referred to in the literature as spiroffite-type phases, after the mineral with a nominal composition Mn<sub>2</sub>Te<sub>3</sub>O<sub>8</sub> (Mandarino et al., 1963a, 1963b). A zinc analogue of spiroffite, the mineral zincspiroffite (Zn<sub>2</sub>Te<sub>3</sub>O<sub>8</sub>), was

\* Corresponding author.

E-mail address: [Juraj.Majzlan@uni-jena.de](mailto:Juraj.Majzlan@uni-jena.de) (J. Majzlan).

<https://doi.org/10.1016/j.chemer.2022.125915>

Received 4 August 2022; Received in revised form 1 October 2022; Accepted 3 October 2022

Available online 7 October 2022

0009-2819/© 2022 The Authors. Published by Elsevier GmbH. This is an open access article under the CC BY license (<http://creativecommons.org/licenses/by/4.0/>).

**Table 1**

Overview of the phases with stoichiometry  $M_2Te_3O_8$ ,  $MTe_6O_{13}$ , and  $MTe_2O_5$  where  $M$  is always a divalent metal cation. Phases investigated in this work by means of calorimetry are marked by arrows. Phases known as minerals are labeled with their name in bold. Additional details on the syntheses can be found in the text.

$M$	$M_2Te_3O_8$	$MTe_6O_{13}$	$MTe_2O_5$
Co	→synthetic	→synthetic	unknown
Cu	synthetic	unknown	→ <b>rajite</b>
Mg	synthetic	→synthetic	synthetic
Mn	<b>spiroffite</b>	synthetic	synthetic
Ni	→synthetic	→synthetic	synthetic
Zn	→ <b>zincspiroffite</b>	synthetic	unknown

described later by Zhang et al. (2004). Further synthetic phases from this group were prepared in the laboratory, namely  $Co_2Te_3O_8$  (Lieder and Gattow, 1969),  $Ni_2Te_3O_8$  (Kolar et al., 1971),  $Cu_2Te_3O_8$  (Feger et al., 1999), and  $Mg_2Te_3O_8$  (Trömel and Ziethen-Reichnack, 1970). They are all isostructural and crystallize in the space group  $C2/c$  (Cooper and Hawthorne, 1996).

Additional phases with the stoichiometry  $M_2Te_3O_8$ , but with a different structure, are known. They house larger  $M^{2+}$  cations and include  $Pb_2Te_3O_8$  (Champarnaud-Mesjard et al., 2001),  $Ca_2Te_3O_8$  (Weil, 2019),  $Sr_2Te_3O_8$  (Elerman and Koçak, 1986), and  $Ba_2Te_3O_8$  (Agarwal and Singh, 2006).

The tellurites with the stoichiometry  $MTe_6O_{13}$  are (so far) unknown from nature but were prepared with different  $M$  cations. These include  $MnTe_6O_{13}$  and  $CoTe_6O_{13}$  (Trömel and Schmid, 1972),  $NiTe_6O_{13}$  (Irvine et al., 2003),  $MgTe_6O_{13}$  (Trömel and Ziethen-Reichnack, 1970), and  $ZnTe_6O_{13}$  (Nawash et al., 2007). They are all isostructural and crystallize in the space group  $R\bar{3}m$ . The phase  $FeTe_6O_{13}$  (van der Lee and Astier, 2007) was reported to crystallize in the space group  $R\bar{3}$  (Shirhanlou and Weil, 2013). The synthesis of a Cu phase from this family was attempted but led only to a mixture of  $TeO_2$  and  $CuTe_2O_5$  (Irvine et al., 2003).

A natural representative of the  $MTe_2O_5$  phases is the mineral rajite ( $CuTe_2O_5$ ) (Williams, 1979). Another, rarer mineral from this group is denningite [(Mn,Zn,Ca)Te<sub>2</sub>O<sub>5</sub>] (Mandarino et al., 1963a, 1963b). Synthetic phases prepared are  $\alpha$ -MnTe<sub>2</sub>O<sub>5</sub> (Miletich, 1993),  $\beta$ -MnTe<sub>2</sub>O<sub>5</sub> and NiTe<sub>2</sub>O<sub>5</sub> (Trömel and Schmid, 1972), and MgTe<sub>2</sub>O<sub>5</sub> (Trömel and Ziethen-Reichnack, 1970). Cobalt or zinc analogues are so far unknown.

The  $MTe_2O_5$  phases are not all isostructural.  $CuTe_2O_5$  crystallizes in the space group  $P2_1/c$  (Williams, 1979),  $NiTe_2O_5$  is orthorhombic with the space group  $Pnma$  (Platte and Trömel, 1981).  $\alpha$ -MnTe<sub>2</sub>O<sub>5</sub> is isostructural with denningite (space group  $P4_2/nbc$ ) (Miletich, 1993) and  $\beta$ -MnTe<sub>2</sub>O<sub>5</sub> is isostructural with MgTe<sub>2</sub>O<sub>5</sub> (space group  $Pbcn$ ) (Johnston and Harrison, 2002).

In this work, we explored the thermodynamics of various  $TeO_2$  phases and metal tellurites. Many synthesis protocols were tediously tested and the pure phases from the few successful runs were used for calorimetric measurements. Enthalpies of formation were determined by acid-solution calorimetry and entropies by relaxation calorimetry.

### 1.1. Note on terminology

There is an unfortunate overlap for the term ‘tellurite’. In mineralogy, this is the name of the mineral tellurite with the composition  $\beta$ - $TeO_2$ . In chemistry, tellurite is a general term for the salts of the tellurous acid,  $H_2TeO_3$ . An example from this work could be the mangano-tellurites  $Mn_2Te_3O_8$ ,  $\beta$ -MnTe<sub>2</sub>O<sub>5</sub>, and  $MnTe_6O_{13}$ . The composition of the anion depends on the degree of polymerization in the structure of a given tellurite phase. There is no easy way to circumvent the problem. In this work, as much as possible, we will use the singular form tellurite for the mineral with composition  $\beta$ - $TeO_2$ . The plural form tellurites or the term tellurite modified by an adjective made of a metal name (e.g., zinc tellurite) will denote the salts of the tellurous acid.

## 2. Materials and methods

For the syntheses, we used tetragonal  $TeO_2$  ( $\alpha$ - $TeO_2$ , Alfa Aesar, 99.99 %), MnO (Alfa Aesar, 99 %), NiO (Alfa Aesar, 99.998 %), MgO (Sigma Aldrich, PhEur), ZnO (Alfa Aesar, 99.999 %),  $CoSO_4 \cdot 7H_2O$  (Merck, ACS),  $NiSO_4 \cdot 7H_2O$  (Acros Organics, for analysis),  $ZnSO_4 \cdot 7H_2O$  (Alfa Aesar, ACS),  $CuSO_4 \cdot 5H_2O$  (Merck, ACS) and  $MnSO_4$  (Chem. Fabrik Dr. Reininghaus, Essen, technical grade). Because of the strong hygroscopic nature of MgO, this chemical was fired for one day at 900 °C before the syntheses.

The orthorhombic  $TeO_2$  ( $\beta$ - $TeO_2$ ) was manufactured by a proprietary technology by Nippon Rare Metal, Inc. The chemical was used as received, without additional treatment.

For the preparation of  $TeO_2$  glass, the starting material was polycrystalline  $\alpha$ - $TeO_2$  (Alfa Aesar, 99.99 %). About 2 g of  $\alpha$ - $TeO_2$  powder were placed in a platinum crucible (ca. 20 cm<sup>3</sup>), the temperature of the furnace was increased at a rate of 50 °C·min<sup>-1</sup> until it reached 900 °C, and the melt was kept at this temperature for 30 min. The crucible was then removed from the furnace and the melt was stirred carefully for a few seconds until it became viscous. Afterwards, quenching took place by dipping quickly, and multiple times, part of the bottom of the platinum crucible in-and-out of water at room temperature. This intermittent quenching technique (*IQ-technique*) is a new and very effective method for producing fairly large samples of pure  $TeO_2$  glass, which are yellow and transparent (Tagiara et al., 2017).

Hydrothermal syntheses were carried out with mixtures of  $\alpha$ - $TeO_2$ , metal (Co, Ni, Mn, Zn, Cu) sulfate, or metal (Ni, Mn, Zn) oxide in deionized water. The pH of the starting solutions was adjusted to a desired value by the addition of 1 %  $H_2SO_4$  or 0.1 M NaOH solution. In the syntheses with the metal sulfates, pH could not be elevated to any selected value. Upon addition of a certain amount of the NaOH solution, a fine precipitate formed in the solution, likely a hydroxide or oxide of the metal present in the solution. In these cases, pH was driven as high as possible before the appearance of the precipitate.

All syntheses were done in Teflon-lined Parr bombs with internal volume of 50 mL. They were filled by 6–12 mL of the initial solution (specified in the separate sections below), tightly closed, and heated at pre-selected temperature for pre-selected time. The products were separated from the remaining solution by filtering through filter paper, washed several times with deionized water, and dried at room temperature.

Samples that contained  $TeO_2$  as the only impurity were washed with 0.1 M NaOH solution to remove  $TeO_2$ . The samples were finely ground and dispersed for 10 min in 30 mL of 0.1 M NaOH solution. Afterwards, they were filtered and washed several times with deionized water. This procedure turned out to be rather efficient for the removal of  $TeO_2$  because its solubility in alkaline solutions is much higher than that of the metal tellurites.

Powder X-ray diffraction (pXRD) data of the solid samples were collected with a Bruker D8 ADVANCE with DAVINCI design, and with  $Cu K\alpha$  radiation, Ni filter, and additionally with a Lynxeye 1D detector. A step size of  $0.02^\circ 2\theta$  and a 0.25 s time per step were used. Lattice parameters were refined using the JANA2006 program (Petříček et al., 2014).

Acid-solution calorimetry on the  $TeO_2$  samples, metal tellurites, and reference compounds was undertaken using an IMC-4400 instrument (Calorimetry Sciences Corporation) (Majzlan, 2017) at the University Jena. A water reservoir was held at a constant temperature of 298.15 K. After stabilization of the calorimeter overnight, the sample pellet with 10 mg weight was dropped into the solvent (25 g 5 N HCl) held in a PEEK (polyetheretherketone) container. The samples dissolved in the acid solution and the heat flow between the sample and reference cell, both immersed in the constant-temperature bath, was measured to calculate the heats of dissolution.

Heat capacity ( $C_p$ ) of selected phases was measured by relaxation calorimetry using a commercial Physical Properties Measurement

**Table 2**

Lattice parameters of the studied compounds. Lattice parameters constrained by symmetry are not listed. Initial structure models: Wyckoff (1963) for  $\alpha$ -TeO<sub>2</sub>, Beyer (1967) for  $\beta$ -TeO<sub>2</sub>, Hanke et al. (1973) for CuTe<sub>2</sub>O<sub>5</sub>, Cooper and Hawthorne (1996) for the M<sub>2</sub>Te<sub>3</sub>O<sub>8</sub> phases, Irvine et al. (2003) for the MTe<sub>6</sub>O<sub>13</sub> phases.

Phase	Space group	Lattice parameters a, b, c [Å] and $\beta$ [°]		V [Å <sup>3</sup> ]
$\alpha$ -TeO <sub>2</sub>	P4 <sub>1</sub> 2 <sub>1</sub> 2	a = 4.8095(1)		176.019 (7)
$\beta$ -TeO <sub>2</sub>	Pbca	c = 7.6096(2)		368.62(3)
		a = 12.0373(4)	c = 5.6033 (2)	
CuTe <sub>2</sub> O <sub>5</sub>	P2 <sub>1</sub> /c	b = 5.4652(3)		459.77(9)
		a = 6.8680(7)	c = 7.6029 (9)	
Zn <sub>2</sub> Te <sub>3</sub> O <sub>8</sub>	C2/c	b = 9.3175(10)		764.79 (12)
		a = 12.6729(13)	$\beta$ = 109.092 (7)	
Ni <sub>2</sub> Te <sub>3</sub> O <sub>8</sub>	C2/c	c = 11.7757 (10)		731.93 (22)
		b = 5.1978(5)	$\beta$ = 99.612 (6)	
Co <sub>2</sub> Te <sub>3</sub> O <sub>8</sub>	C2/c	c = 11.4992 (19)		759.32 (24)
		a = 12.3846(19)	$\beta$ = 98.700 (11)	
CoTe <sub>6</sub> O <sub>13</sub>	R-3m	c = 11.6260 (26)		1698.74 (9)
		b = 5.2106(8)	$\beta$ = 98.896 (9)	
NiTe <sub>6</sub> O <sub>13</sub>	R-3m	a = 10.1646(3)		1682.67 (17)
		a = 10.1479(5)	c = 18.9866 (7)	
MgTe <sub>6</sub> O <sub>13</sub>	R-3m	c = 18.8676 (14)		1701.89 (8)
		a = 10.1760(3)	c = 18.9779 (6)	

**Table 3**

Summary of the synthesis conditions and reaction products for the cobalt tellurites. The source of cobalt in all these syntheses was CoSO<sub>4</sub>, the synthesis time was always 3 days.

Sample	T [°C]	pH	Products (in order of decreasing abundance)
Co_pH3_170	170	3	Co <sub>2</sub> Te <sub>3</sub> O <sub>8</sub> , TeO <sub>2</sub>
Co_pH6_170	170	6	Co <sub>2</sub> Te <sub>3</sub> O <sub>8</sub> , TeO <sub>2</sub>
Co_pH75_170	170	7.5	Co <sub>2</sub> Te <sub>3</sub> O <sub>8</sub> , TeO <sub>2</sub>
Co_pH6_200	200	6	Co <sub>2</sub> Te <sub>3</sub> O <sub>8</sub> , CoTe <sub>6</sub> O <sub>13</sub> , TeO <sub>2</sub>
Co_pH3_230	230	3	CoTe <sub>6</sub> O <sub>13</sub> , Co <sub>2</sub> Te <sub>3</sub> O <sub>8</sub> , TeO <sub>2</sub> , unknown
Co_pH6_230	230	6	CoTe <sub>6</sub> O <sub>13</sub> , Co <sub>2</sub> Te <sub>3</sub> O <sub>8</sub> , TeO <sub>2</sub>
Co_pH75_230	230	7.5	CoTe <sub>6</sub> O <sub>13</sub> , Co <sub>2</sub> Te <sub>3</sub> O <sub>8</sub> , TeO <sub>2</sub>

System (PPMS, from Quantum Design, San Diego, California). With due care, the accuracy can be within 1 % from 5 K to 300 K, and 5 % from 0.7 K to 5 K (Kennedy et al. 2007). Powdered samples were wrapped in a thin Al foil and compressed to produce an about 0.5 mm thick pellet which was then placed onto the sample platform of the calorimeter for measurement. The heat capacity was measured in the PPMS in a 2 to 300 K temperature interval.

### 3. Results

#### 3.1. Tellurium oxides

The TeO<sub>2</sub> samples ( $\alpha$  and  $\beta$ ) were used as received. Their X-ray diffraction patterns contained only the sharp peaks of one of the polymorphs. The refined lattice parameters are listed in Table 2. The pXRD pattern of the TeO<sub>2</sub> glass showed only a broad feature of elevated background, centered at 27.5 °2 $\theta$ . No diffraction peaks were observed in this pattern.

#### 3.2. Cobalt tellurites

For the hydrothermal syntheses, 0.3 g TeO<sub>2</sub> and 12 mL of 0.5 M CoSO<sub>4</sub> solution were used. The syntheses were carried out at temperatures 170, 200, and 230 °C at pH values of 3, 6, or 7.5 for 3 days. The results are summarized in Table 3.

At 170 °C, all samples consisted of round, deep purple crystal aggregates with sizes 0.1–0.2 mm, mixed with the remaining powdery TeO<sub>2</sub>. The purple aggregates are sometimes intergrown with minute colorless crystals of TeO<sub>2</sub>. These aggregates were separated from the rest of the sample under binocular microscope. The remaining TeO<sub>2</sub> was removed by washing in 0.1 M NaOH solution, resulting in a pure Co<sub>2</sub>Te<sub>3</sub>O<sub>8</sub> sample (Fig. 1).

The syntheses at 200 or 230 °C also produced such deep purple aggregates, together with powdery TeO<sub>2</sub>. An additional phase was represented by purple rhombohedral crystals that reached the size of 1.5 mm in the synthesis at 230 °C and pH 3 or 6. They were easily separated under binocular microscope and were shown to be pure CoTe<sub>6</sub>O<sub>13</sub> (Fig. 1).

A comparison of our results and those previously published shows how sensitive these syntheses are to temperature, pH, and composition of the starting chemicals. Lieder and Gattow (1969) reported on synthesis of Co<sub>2</sub>Te<sub>3</sub>O<sub>8</sub> with K<sub>2</sub>TeO<sub>3</sub> and CoSO<sub>4</sub> at pH 6 and 300–310 °C, but mentioned no CoTe<sub>6</sub>O<sub>13</sub> or another Co tellurite phase. On the other hand, Irvine et al. (2003) synthesized 2 mm large CoTe<sub>6</sub>O<sub>13</sub> crystals at 155 °C from CoCl<sub>2</sub>, TeO<sub>2</sub>, and BaCO<sub>3</sub>.

#### 3.3. Nickel tellurites

For the hydrothermal syntheses with nickel sulfate, 0.3 g TeO<sub>2</sub> and 12 mL of 0.5 M NiSO<sub>4</sub> solution were used. Temperatures, pH values, and reaction times are summarized in Table 4. For the hydrothermal syntheses with NiO, we always used 1 mmol (0.1596 g) of TeO<sub>2</sub>, together with 0.167 mmol (0.0125 g) NiO, 0.5 mmol (0.0374 g) NiO, or 0.667 mmol (0.0498 g) NiO. These amounts correspond to molar Ni/Te ratios of 1:6, 1:2, and 2:3. These ratios are also specified in the sample labels in Table 4. For the syntheses with oxides, the starting chemicals were finely ground and mixed in an agate mortar, then mixed with 10 mL of deionized water and loaded into the pressure bombs.

In the syntheses at 170 °C, no tellurites were produced. Even after 8 days, TeO<sub>2</sub> did not appear to undergo any change. The products contained a small amount of crystalline nickel sulfate, identified as NiSO<sub>4</sub>·4H<sub>2</sub>O after washing and drying.

At 230 °C, tellurites formed as the dominant phases in the synthesis products. At pH 6 and 7.5, the products were yellowish green and consisted of Ni<sub>2</sub>Te<sub>3</sub>O<sub>8</sub>, TeO<sub>2</sub>, NiSO<sub>4</sub>·H<sub>2</sub>O. More Ni<sub>2</sub>Te<sub>3</sub>O<sub>8</sub> was produced at pH 7.5. At pH 3, the product consisted of light green powder (mixture of NiSO<sub>4</sub>·H<sub>2</sub>O, and TeO<sub>2</sub>) with radial aggregates of brownish green acicular crystals, up to 0.4 mm large, and orange rhombohedral crystals with size up to 0.2 mm. The orange crystals were separated under binocular microscope and were pure NiTe<sub>6</sub>O<sub>13</sub> (Fig. 1). The brownish green aggregates were also separated and those contaminated by attached NiTe<sub>6</sub>O<sub>13</sub> crystals were discarded. The remaining sample was gently ground and washed with 0.1 M NaOH solution to remove TeO<sub>2</sub>. The resulting sample was pure Ni<sub>2</sub>Te<sub>3</sub>O<sub>8</sub> (Fig. 1).

The hydrothermal syntheses with the initial oxides always produced yellowish green powders. They are a mixture of Ni<sub>2</sub>Te<sub>3</sub>O<sub>8</sub> and TeO<sub>2</sub>. Increasing of the Ni/Te ratio leads to increasing of the proportion of Ni<sub>2</sub>Te<sub>3</sub>O<sub>8</sub> in the samples.

In summary, our methods yielded tellurites only at 230 °C. The best results were achieved at pH 3. In this sample, the individual phases were large enough to be separated under microscope and purified by the treatment in 0.1 M NaOH solution, if needed. Otherwise, the syntheses always gave mixtures; in powdery, fine-grained form, such mixtures are not suitable for calorimetric experiments. Feger et al. (1999) described a hydrothermal route for the synthesis of Ni<sub>2</sub>Te<sub>3</sub>O<sub>8</sub> with NiO and TeO<sub>2</sub> in a

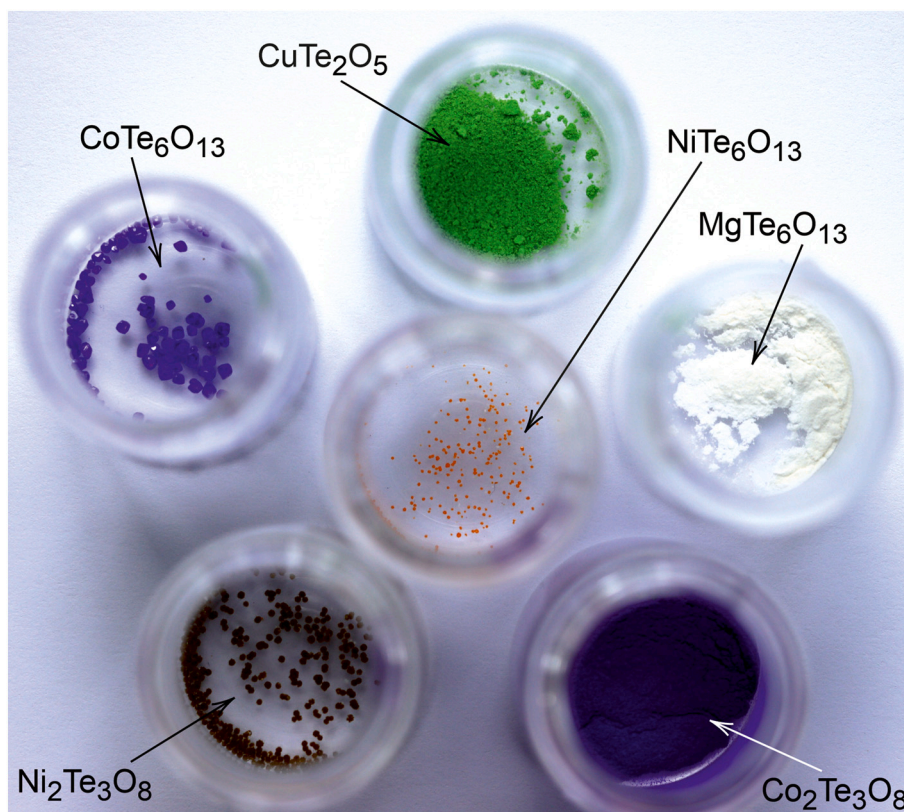


**Fig. 1.** Some metal tellurites for the calorimetric experiments. Some of the samples consist of larger crystals, some of them are powdery. Note the vivid colors in the phases with transition metals.

**Table 4**

Summary of the synthesis conditions and reaction products for the nickel tellurites.

Sample	T [°C]	pH	t [days]	Ni source	Products (in order of decreasing abundance)
Ni_pH3_170	170	3	3	Sulfate	TeO <sub>2</sub> , NiSO <sub>4</sub> ·4H <sub>2</sub> O
Ni_pH6_170_d3	170	6	3	Sulfate	TeO <sub>2</sub> , NiSO <sub>4</sub> ·4H <sub>2</sub> O
Ni_pH6_170_d8	170	6	8	Sulfate	TeO <sub>2</sub>
Ni_pH75_170	170	7.5	3	Sulfate	TeO <sub>2</sub> , NiSO <sub>4</sub> ·4H <sub>2</sub> O
Ni_pH3_230	230	3	3	Sulfate	NiTe <sub>6</sub> O <sub>13</sub> , Ni <sub>2</sub> Te <sub>3</sub> O <sub>8</sub> , TeO <sub>2</sub> , NiSO <sub>4</sub> ·H <sub>2</sub> O
Ni_pH6_230	230	6	3	Sulfate	Ni <sub>2</sub> Te <sub>3</sub> O <sub>8</sub> , TeO <sub>2</sub> , NiSO <sub>4</sub> ·H <sub>2</sub> O
Ni_pH75_230	230	7.5	3	Sulfate	Ni <sub>2</sub> Te <sub>3</sub> O <sub>8</sub> , TeO <sub>2</sub> , NiSO <sub>4</sub> ·H <sub>2</sub> O
1NiO_6TeO2_hydr	230	7	7	Oxide	Ni <sub>2</sub> Te <sub>3</sub> O <sub>8</sub> , TeO <sub>2</sub>
1NiO_2TeO2_hydr	230	7	7	Oxide	Ni <sub>2</sub> Te <sub>3</sub> O <sub>8</sub> , TeO <sub>2</sub>
2NiO_3TeO2_hydr	230	7	7	Oxide	Ni <sub>2</sub> Te <sub>3</sub> O <sub>8</sub> , TeO <sub>2</sub>

NH<sub>4</sub>Cl solution at 375 °C. To our best knowledge, there is only one synthesis of NiTe<sub>6</sub>O<sub>13</sub> reported so far; Irvine et al. (2003) prepared this phase at 155 °C from TeO<sub>2</sub>, NiCl<sub>2</sub>·6H<sub>2</sub>O, and BaCO<sub>3</sub>. Solid-state syntheses of Irvine et al. (2003) led to the formation of a mixture of NiTe<sub>2</sub>O<sub>5</sub> and TeO<sub>2</sub>.

### 3.4. Manganese tellurites

Syntheses of manganese tellurites were attempted hydrothermally, from sulfates or oxides. The results are summarized in Table 5. For the hydrothermal syntheses with sulfates, the charges consisted of 0.2 g TeO<sub>2</sub> and 8 mL of 0.5 M MnSO<sub>4</sub> solution. For the syntheses with MnO, 1 mmol TeO<sub>2</sub> (0.1596 g) was mixed with 0.167 mmol (0.0118 g) MnO, 0.5 mmol (0.0355 g) MnO, or 0.667 mmol (0.0473 g) MnO, corresponding

**Table 5**

Summary of the synthesis conditions and reaction products for the manganese tellurites.

Sample	T [°C]	pH	t [days]	Mn source	Products (in order of decreasing abundance)
Mn_H2SO4_170	170	2.5	3	Sulfate	Mn <sub>2</sub> Te <sub>3</sub> O <sub>8</sub> , β-MnTe <sub>2</sub> O <sub>5</sub> , TeO <sub>2</sub> , MnSO <sub>4</sub> ·H <sub>2</sub> O
Mn_unv_170	170	2.8	3	Sulfate	Mn <sub>2</sub> Te <sub>3</sub> O <sub>8</sub> , β-MnTe <sub>2</sub> O <sub>5</sub> , TeO <sub>2</sub> , MnSO <sub>4</sub> ·H <sub>2</sub> O
Mn_NaOH_170	170	5	3	Sulfate	TeO <sub>2</sub> , Mn <sub>2</sub> (TeO <sub>3</sub> )(SO <sub>4</sub> )(H <sub>2</sub> O)
Mn_H2SO4_230	230	2.5	3	Sulfate	Mn <sub>2</sub> Te <sub>3</sub> O <sub>8</sub> , β-MnTe <sub>2</sub> O <sub>5</sub> , TeO <sub>2</sub>
Mn_unv_230	230	2.8	3	Sulfate	TeO <sub>2</sub> , Mn <sub>2</sub> Te <sub>3</sub> O <sub>8</sub>
Mn_NaOH_230	230	5	3	Sulfate	TeO <sub>2</sub> , Mn <sub>2</sub> Te <sub>3</sub> O <sub>8</sub> , Mn <sub>2</sub> (TeO <sub>3</sub> )(SO <sub>4</sub> )(H <sub>2</sub> O)
2MnO_3TeO2_hydr	230	7	7	Oxide	Mn <sub>2</sub> Te <sub>3</sub> O <sub>8</sub> , MnTe <sub>6</sub> O <sub>13</sub> , β-MnTe <sub>2</sub> O <sub>5</sub>
1MnO_2TeO2_hydr	230	7	7	Oxide	Mn <sub>2</sub> Te <sub>3</sub> O <sub>8</sub> , MnTe <sub>6</sub> O <sub>13</sub> , β-MnTe <sub>2</sub> O <sub>5</sub> , MnO
1MnO_6TeO2_hydr	230	7	7	Oxide	MnTe <sub>6</sub> O <sub>13</sub> , TeO <sub>2</sub> , MnO

to molar Mn/Te ratios of 1:6, 1:2, and 2:3. These ratios are also specified in the sample labels in Table 5.

The products of these syntheses are usually powdery, some of them with pinkish brown aggregates with size up to 0.5 mm. In all cases, the samples consisted of multiple phases that could not be mechanically separated from each other. The sample Mn\_unv\_230 gave a mixture of TeO<sub>2</sub> and Mn<sub>2</sub>Te<sub>3</sub>O<sub>8</sub> but TeO<sub>2</sub> was by far the dominant phase and separation of Mn<sub>2</sub>Te<sub>3</sub>O<sub>8</sub> was not feasible. Of interest for further investigation is the mixed tellurite-sulfate Mn<sub>2</sub>(TeO<sub>3</sub>)(SO<sub>4</sub>)(H<sub>2</sub>O).

**Table 6**

Summary of the synthesis conditions and reaction products for the zinc tellurites.

Sample	T [°C]	pH	t [days]	Zn source	Products (in order of decreasing abundance)
Zn_H2SO4_170	170	3	3	Sulfate	Zn <sub>2</sub> Te <sub>3</sub> O <sub>8</sub> , TeO <sub>2</sub>
Zn_unv_170	170	4.3	3	Sulfate	Zn <sub>2</sub> Te <sub>3</sub> O <sub>8</sub> , TeO <sub>2</sub>
Zn_NaOH_170	170	5.75	3	Sulfate	Zn <sub>2</sub> Te <sub>3</sub> O <sub>8</sub> , TeO <sub>2</sub>
Zn_H2SO4_230	230	3	3	Sulfate	Zn <sub>2</sub> Te <sub>3</sub> O <sub>8</sub> , TeO <sub>2</sub>
Zn_unv_230	230	4.3	3	Sulfate	TeO <sub>2</sub> , Zn <sub>2</sub> Te <sub>3</sub> O <sub>8</sub>
Zn_NaOH_230	230	5.75	3	Sulfate	Zn <sub>2</sub> Te <sub>3</sub> O <sub>8</sub> , TeO <sub>2</sub> , ZnSO <sub>4</sub> ·7H <sub>2</sub> O
2ZnO_3TeO2_d7_hydr	230	7	7	Oxide	Zn <sub>2</sub> Te <sub>3</sub> O <sub>8</sub> , ZnTeO <sub>3</sub> , TeO <sub>2</sub>

**Table 7**

Summary of the synthesis conditions and reaction products for the copper tellurites. All runs lasted 3 days.

Sample	T [°C]	CuSO4 solution	TeO <sub>2</sub> (grams)	Products (in order of decreasing abundance)
Cu_0,5M_170	170	0.5 M, 6 mL	0.1	CuTe <sub>2</sub> O <sub>5</sub> , TeO <sub>2</sub> , unknown
Cu_0,5M_230	230	0.5 M, 6 mL	0.1	CuTe <sub>2</sub> O <sub>5</sub> , TeO <sub>2</sub> , Cu <sub>3</sub> SO <sub>4</sub> (OH) <sub>4</sub> , Cu <sub>7</sub> (TeO <sub>3</sub> ) <sub>2</sub> (SO <sub>4</sub> ) <sub>2</sub> (OH) <sub>6</sub>
Cu_0,3M_230	230	0.3 M, 10 mL	0.1	CuTe <sub>2</sub> O <sub>5</sub> , TeO <sub>2</sub> , unknown
Cu_0,1M_230	230	0.1 M, 10 mL	0.1596 (1 mmol)	CuTe <sub>2</sub> O <sub>5</sub> , TeO <sub>2</sub>

In summary, our products contained the targeted phases but they could not be separated from other phases. Irvine et al. (2003) succeeded to synthesize MnTe<sub>6</sub>O<sub>13</sub> with BaCO<sub>3</sub>, TeO<sub>2</sub>, and MnCl<sub>2</sub>·4H<sub>2</sub>O at 200 °C and the Mn/Te ratio of 1:3, with only a minor TeO<sub>2</sub> impurity. A similar synthesis was mentioned by Johnston and Harrison (2002) at 180 °C and Mn/Te ratio of 2:3. They obtained β-MnTe<sub>2</sub>O<sub>5</sub> and additional crystalline phases. It appears that MnSO<sub>4</sub> disturbs the syntheses and an alternative source of Mn should be considered, if such syntheses should be attempted in the future.

### 3.5. Zinc tellurites

The syntheses of zinc tellurites were attempted by the hydrothermal route from TeO<sub>2</sub> and ZnSO<sub>4</sub>·7H<sub>2</sub>O or TeO<sub>2</sub> and ZnO. For the first way, 0.2 g TeO<sub>2</sub> and 8 mL of 0.5 M ZnSO<sub>4</sub> solution were mixed and heated at the temperature, pH, and time specified in Table 6. For the synthesis with ZnO, 1 mmol (0.1596 g) TeO<sub>2</sub> and 0.667 mmol (0.0542 g) ZnO (Zn:Te = 2:3) were mixed in a mortar and homogenized. The mixture was placed in a Teflon-lined bomb with 10 mL of deionized water (Table 6).

The hydrothermal syntheses with TeO<sub>2</sub> and ZnSO<sub>4</sub> produced white or yellowish powders at both temperatures used. All these samples consisted of Zn<sub>2</sub>Te<sub>3</sub>O<sub>8</sub> and TeO<sub>2</sub>. TeO<sub>2</sub> is the dominant product in the run at 230 °C at pH = 4.3 (pH without addition of H<sub>2</sub>SO<sub>4</sub> or NaOH). At pH of 5.75, the phase Zn<sub>2</sub>Te<sub>3</sub>O<sub>8</sub> is much more abundant. Sulfate from the parental solution does not influence the products except for the sample Zn\_NaOH\_230 with small amount of ZnSO<sub>4</sub>·7H<sub>2</sub>O.

The yield of Zn<sub>2</sub>Te<sub>3</sub>O<sub>8</sub> increases with falling temperature and rising pH value of the parental solution. The only impurity is TeO<sub>2</sub> which can be removed by the treatment with NaOH. In future studies, even lower synthesis temperatures could perhaps lead to pure Zn<sub>2</sub>Te<sub>3</sub>O<sub>8</sub> samples.

The synthesis with TeO<sub>2</sub> and ZnO produced off-white powder that consisted of Zn<sub>2</sub>Te<sub>3</sub>O<sub>8</sub>, ZnTeO<sub>3</sub>, and TeO<sub>2</sub>. The ZnTeO<sub>3</sub> phase cannot be separated from the sample. The synthesis products from ZnO, TeO<sub>2</sub>, and NH<sub>4</sub>Cl at 375 °C (Feger et al., 1999) were also reported to contain a small amount of ZnTeO<sub>3</sub>. To our best knowledge, the synthesis of a ZnTe<sub>2</sub>O<sub>5</sub> phase was not yet described. ZnTe<sub>6</sub>O<sub>13</sub> was prepared by

**Table 8**

Summary of the hydrothermal synthesis conditions and reaction products for the magnesium tellurites. The source of magnesium in all these syntheses was MgO. All runs lasted 3 days.

Sample	T [°C]	pH	Products (in order of decreasing abundance)
2MgO_3TeO2_HCl_170	170	2.5	Mg <sub>2</sub> Te <sub>3</sub> O <sub>8</sub> , MgTe <sub>2</sub> O <sub>5</sub> , TeO <sub>2</sub> , Mg <sub>5</sub> O <sub>4</sub> (OH) <sub>2</sub>
2MgO_3TeO2_H2O_170	170	7	Mg <sub>2</sub> Te <sub>3</sub> O <sub>8</sub> , MgTe <sub>2</sub> O <sub>5</sub> , Mg <sub>5</sub> O <sub>4</sub> (OH) <sub>2</sub>
2MgO_3TeO2_NaOH_170	170	11.7	Mg <sub>2</sub> Te <sub>3</sub> O <sub>8</sub> , MgTe <sub>2</sub> O <sub>5</sub> , Mg <sub>5</sub> O <sub>4</sub> (OH) <sub>2</sub>
2MgO_3TeO2_HCl_230	230	2.5	Mg <sub>2</sub> Te <sub>3</sub> O <sub>8</sub> , MgTe <sub>2</sub> O <sub>5</sub> , TeO <sub>2</sub>
2MgO_3TeO2_H2O_230	230	7	Mg <sub>2</sub> Te <sub>3</sub> O <sub>8</sub> , MgTe <sub>2</sub> O <sub>5</sub> , Mg <sub>5</sub> O <sub>4</sub> (OH) <sub>2</sub>
2MgO_3TeO2_NaOH_230	230	11.7	Mg <sub>2</sub> Te <sub>3</sub> O <sub>8</sub> , MgTe <sub>2</sub> O <sub>5</sub> , TeO <sub>2</sub> , Mg <sub>5</sub> O <sub>4</sub> (OH) <sub>2</sub>

repeated melting and cooling of a starting mixture under stream of oxygen (Nawash et al., 2007).

### 3.6. Copper tellurites

Hydrothermal syntheses of copper tellurites were carried out with CuSO<sub>4</sub> solutions and TeO<sub>2</sub>. The amount and molarity of the CuSO<sub>4</sub> solution and the mass of TeO<sub>2</sub> is specified in Table 7. In these syntheses, the pH was not adjusted because that could lead to precipitation of copper sulfates.

The synthesis with 0.1 M CuSO<sub>4</sub> solution yielded a light green powder composed of CuTe<sub>2</sub>O<sub>5</sub> and a minor amount TeO<sub>2</sub>. The TeO<sub>2</sub> impurity was removed by washing with NaOH solution and this sample was used for calorimetry (Fig. 1). The syntheses with 0.5 M and 0.3 M CuSO<sub>4</sub> solutions yielded a light green powder with round, dark green aggregates of size up to 1 mm. These aggregates are made of several phases specified in Table 7. The phases other than CuTe<sub>2</sub>O<sub>5</sub> and TeO<sub>2</sub> included antlerite [Cu<sub>3</sub>SO<sub>4</sub>(OH)<sub>4</sub>], a copper tellurite-sulfate, and one other phase or phases whose diffraction peaks did not match with any record in the database.

### 3.7. Magnesium tellurites

For the hydrothermal syntheses of the magnesium tellurites, 1.5 mmol (0.2394 g) of TeO<sub>2</sub> and 1 mmol (0.0403 g) MgO was used (Lin et al., 2013). The oxides were thoroughly mixed, suspended in 10 mL of deionized water, and treated at a selected temperature in a Teflon-lined Parr bomb. The run conditions are specified in Table 8. None of the syntheses yielded a phase-pure sample of one magnesium tellurite or such sample contaminated only by TeO<sub>2</sub>. The samples were off-white, powdery, and the separation of the individual phases under a binocular microscope was not possible.

Solid-state syntheses were attempted to synthesize MgTe<sub>2</sub>O<sub>5</sub> and MgTe<sub>6</sub>O<sub>13</sub> after the procedures outlined in Trömel and Zithen-Reichnack (1970). For the synthesis of MgTe<sub>6</sub>O<sub>13</sub>, MgO and TeO<sub>2</sub> were mixed in stoichiometric molar proportion of 1:6, homogenized, and heated for 60 h at 610 °C in air. For MgTe<sub>2</sub>O<sub>5</sub>, Mg/Te molar ratios (as mixtures of MgO and TeO<sub>2</sub>) of 1:2, 1:1.9, 1:1.85, and 1:8 were tested. The oxide mixtures were homogenized and heated for 24 h at 680 °C.

The solid-state synthesis that targeted MgTe<sub>6</sub>O<sub>13</sub> produced white powder with an impurity of TeO<sub>2</sub>. This impurity was removed by washing in 0.1 M NaOH, thus yielding a pure MgTe<sub>6</sub>O<sub>13</sub> sample that was used for calorimetry (Fig. 1). The refined lattice parameters are listed in Table 2. The syntheses that targeted MgTe<sub>2</sub>O<sub>5</sub> produced always mixtures of the desired phase with MgTe<sub>6</sub>O<sub>13</sub> or Mg<sub>3</sub>TeO<sub>6</sub>. None of the products was suitable for calorimetric investigation.

### 3.8. Acid-solution calorimetry

Several phase-pure samples of metal tellurites were selected for acid-solution calorimetry (Table 1). All samples, including the TeO<sub>2</sub> phases,

**Table 9**

Thermochemical cycles for the calculation of the formation enthalpies of the studied compounds. The enthalpies of dissolution in the calorimetric solvent (5 N HCl) are listed in the lower part of the table. All dissolution enthalpies measured at  $T = 298.15$  K.

$\alpha\text{-TeO}_2$ (cr) + $\text{H}_2\text{O}$ (aq) $\rightarrow$ $\text{TeO}_3^{2-}$ (aq) + $2\text{H}^+$ (aq)	1 $\alpha$
$\beta\text{-TeO}_2$ (cr) + $\text{H}_2\text{O}$ (aq) $\rightarrow$ $\text{TeO}_3^{2-}$ (aq) + $2\text{H}^+$ (aq)	1 $\beta$
$\text{TeO}_2$ (glass) + $\text{H}_2\text{O}$ (aq) $\rightarrow$ $\text{TeO}_3^{2-}$ (aq) + $2\text{H}^+$ (aq)	1g
$\text{CuO}$ (cr) + $2\text{H}^+$ (aq) $\rightarrow$ $\text{Cu}^{2+}$ (aq) + $\text{H}_2\text{O}$ (aq)	2
$\text{ZnO}$ (cr) + $2\text{H}^+$ (aq) $\rightarrow$ $\text{Zn}^{2+}$ (aq) + $\text{H}_2\text{O}$ (aq)	3
$\text{MgO}$ (cr) + $2\text{H}^+$ (aq) $\rightarrow$ $\text{Mg}^{2+}$ (aq) + $\text{H}_2\text{O}$ (aq)	4
$\text{MgSO}_4$ (cr) $\rightarrow$ $\text{Mg}^{2+}$ (aq) + $\text{SO}_4^{2-}$ (aq)	5
$\text{NiSO}_4 \cdot 7\text{H}_2\text{O}$ (cr) $\rightarrow$ $\text{Ni}^{2+}$ (aq) + $\text{SO}_4^{2-}$ (aq) + $7\text{H}_2\text{O}$ (aq)	6
$\text{CoSO}_4 \cdot 7\text{H}_2\text{O}$ (cr) $\rightarrow$ $\text{Co}^{2+}$ (aq) + $\text{SO}_4^{2-}$ (aq) + $7\text{H}_2\text{O}$ (aq)	7
$\text{H}_2\text{O}$ (l) $\rightarrow$ $\text{H}_2\text{O}$ (aq)	8
$\text{CuTe}_2\text{O}_5$ (cr) + $\text{H}_2\text{O}$ (aq) $\rightarrow$ $\text{Cu}^{2+}$ (aq) + $2\text{TeO}_3^{2-}$ (aq) + $2\text{H}^+$ (aq)	9
$\text{Zn}_2\text{Te}_3\text{O}_8$ (cr) + $\text{H}_2\text{O}$ (aq) $\rightarrow$ $2\text{Zn}^{2+}$ (aq) + $3\text{TeO}_3^{2-}$ (aq) + $2\text{H}^+$ (aq)	10
$\text{Co}_2\text{Te}_3\text{O}_8$ (cr) + $\text{H}_2\text{O}$ (aq) $\rightarrow$ $2\text{Co}^{2+}$ (aq) + $3\text{TeO}_3^{2-}$ (aq) + $2\text{H}^+$ (aq)	11
$\text{MgTe}_6\text{O}_{13}$ (cr) + $5\text{H}_2\text{O}$ (aq) $\rightarrow$ $\text{Mg}^{2+}$ (aq) + $6\text{TeO}_3^{2-}$ (aq) + $10\text{H}^+$ (aq)	12
$\text{NiTe}_6\text{O}_{13}$ (cr) + $5\text{H}_2\text{O}$ (aq) $\rightarrow$ $\text{Ni}^{2+}$ (aq) + $6\text{TeO}_3^{2-}$ (aq) + $10\text{H}^+$ (aq)	13
$\text{CoTe}_6\text{O}_{13}$ (cr) + $5\text{H}_2\text{O}$ (aq) $\rightarrow$ $\text{Co}^{2+}$ (aq) + $6\text{TeO}_3^{2-}$ (aq) + $10\text{H}^+$ (aq)	14
$\text{Te}$ (cr) + $\text{O}_2$ (g) $\rightarrow$ $\alpha\text{-TeO}_2$ (cr)	15 $\alpha$
$\text{Te}$ (cr) + $\text{O}_2$ (g) $\rightarrow$ $\beta\text{-TeO}_2$ (cr)	15 $\beta$
$\text{Te}$ (cr) + $\text{O}_2$ (g) $\rightarrow$ $\text{TeO}_2$ (glass)	15g
$\text{Cu}$ (cr) + $0.5\text{O}_2$ (g) $\rightarrow$ $\text{CuO}$ (cr)	16
$\text{Zn}$ (cr) + $0.5\text{O}_2$ (g) $\rightarrow$ $\text{ZnO}$ (cr)	17
$\text{Mg}$ (cr) + $0.5\text{O}_2$ (g) $\rightarrow$ $\text{MgO}$ (cr)	18
$\text{Mg}$ (cr) + $\text{S}$ (cr) + $2\text{O}_2$ (g) $\rightarrow$ $\text{MgSO}_4$ (cr)	19
$\text{Ni}$ (cr) + $\text{S}$ (cr) + $5.5\text{O}_2$ (g) + $7\text{H}_2$ (g) $\rightarrow$ $\text{NiSO}_4 \cdot 7\text{H}_2\text{O}$ (cr)	20
$\text{Co}$ (cr) + $\text{S}$ (cr) + $5.5\text{O}_2$ (g) + $7\text{H}_2$ (g) $\rightarrow$ $\text{CoSO}_4 \cdot 7\text{H}_2\text{O}$ (cr)	21
$\text{H}_2$ (g) + $0.5\text{O}_2$ (g) $\rightarrow$ $\text{H}_2\text{O}$ (l)	22
$\text{Cu}$ (cr) + $2\text{Te}$ (cr) + $2.5\text{O}_2$ (g) $\rightarrow$ $\text{CuTe}_2\text{O}_5$ (cr)	23
$2\text{Zn}$ (cr) + $3\text{Te}$ (cr) + $4\text{O}_2$ (g) $\rightarrow$ $\text{Zn}_2\text{Te}_3\text{O}_8$ (cr)	24
$2\text{Co}$ (cr) + $3\text{Te}$ (cr) + $4\text{O}_2$ (g) $\rightarrow$ $\text{Co}_2\text{Te}_3\text{O}_8$ (cr)	25
$\text{Mg}$ (cr) + $6\text{Te}$ (cr) + $6.5\text{O}_2$ (g) $\rightarrow$ $\text{MgTe}_6\text{O}_{13}$ (cr)	26
$\text{Ni}$ (cr) + $6\text{Te}$ (cr) + $6.5\text{O}_2$ (g) $\rightarrow$ $\text{NiTe}_6\text{O}_{13}$ (cr)	27
$\text{Co}$ (cr) + $6\text{Te}$ (cr) + $6.5\text{O}_2$ (g) $\rightarrow$ $\text{CoTe}_6\text{O}_{13}$ (cr)	28
$\Delta_{\text{diss}}\text{H}$ [kJ·mol <sup>-1</sup> ]	$\Delta_{\text{f}}\text{H}^\circ$ [kJ·mol <sup>-1</sup> ]
$\Delta\text{H}_{1\alpha} = 6.30 \pm 0.05^{(7)\text{f}}$	$\Delta\text{H}_{15\alpha} = -322.0 \pm 1.3^{\text{d}}$
$\Delta\text{H}_{1\beta} = 4.90 \pm 0.05(4)$	$\Delta\text{H}_{1\alpha} - \Delta\text{H}_{1\beta} + \Delta\text{H}_{15\alpha}$
$\Delta\text{H}_{1g} = -7.79 \pm 0.10(4)$	
$\Delta\text{H}_2 = -51.53 \pm 0.16$	$\Delta\text{H}_{16} = -156.1 \pm 2.0^{\text{e}}$
$\Delta\text{H}_3 = -70.24 \pm 0.11$	$\Delta\text{H}_{17} = -350.5 \pm 0.3^{\text{e}}$
$\Delta\text{H}_4 = -149.68 \pm 0.60$	$\Delta\text{H}_{18} = -601.6 \pm 0.3^{\text{e}}$
$\Delta\text{H}_5 = -53.50 \pm 0.48$	$\Delta\text{H}_{19} = -1288.64 \pm 1.28^{\text{f}}$
$\Delta\text{H}_6 = 41.26 \pm 0.58$	$\Delta\text{H}_{20} = -2976.8 \pm 1.5^{\text{g}}$
$\Delta\text{H}_7 = 44.66 \pm 0.31$	$\Delta\text{H}_{21} = -2979.3 \pm 1.5^{\text{g}}$
$\Delta\text{H}_8 = -0.54$	$\Delta\text{H}_{22} = -285.8 \pm 0.1^{\text{e}}$
$\Delta\text{H}_9 = -18.79 \pm 0.45(4)$	$\Delta\text{H}_{23} = 2\Delta\text{H}_{1\alpha} + \Delta\text{H}_2 - \Delta\text{H}_9 + 2\Delta\text{H}_{15\alpha} + \Delta\text{H}_{16}$
$\Delta\text{H}_{10} = -66.05 \pm 0.62$	

**Table 9 (continued)**

$\Delta\text{H}_{11} = -111.68 \pm 0.64$	$\Delta\text{H}_{24} = 3\Delta\text{H}_{1\alpha} + 2\Delta\text{H}_3 - \Delta\text{H}_{10} + 3\Delta\text{H}_{15\alpha} + 2\Delta\text{H}_{17}$
$\Delta\text{H}_{12} = -119.69 \pm 0.88$	$\Delta\text{H}_{25} = 3\Delta\text{H}_{1\alpha} + 2\Delta\text{H}_7 + 2\Delta\text{H}_4 - \Delta\text{H}_{11} - 2\Delta\text{H}_5 - 14\Delta\text{H}_8 + 2\Delta\text{H}_{21} + 3\Delta\text{H}_{15\alpha} + 2\Delta\text{H}_{18} - 2\Delta\text{H}_{19} - 14\Delta\text{H}_{22}$
$\Delta\text{H}_{13} = -35.72 \pm 0.34$	$\Delta\text{H}_{26} = 6\Delta\text{H}_{1\alpha} + \Delta\text{H}_4 - \Delta\text{H}_{12} + 6\Delta\text{H}_{15\alpha} + \Delta\text{H}_{18}$
$\Delta\text{H}_{14} = -21.13 \pm 0.12$	$\Delta\text{H}_{27} = 6\Delta\text{H}_{1\alpha} + \Delta\text{H}_6 + \Delta\text{H}_4 - \Delta\text{H}_{13} - \Delta\text{H}_5 - 7\Delta\text{H}_8 + 6\Delta\text{H}_{15\alpha} + \Delta\text{H}_{20} + \Delta\text{H}_{18} - \Delta\text{H}_{19} - 7\Delta\text{H}_{22}$
	$\Delta\text{H}_{28} = 6\Delta\text{H}_{1\alpha} + \Delta\text{H}_7 + \Delta\text{H}_4 - \Delta\text{H}_{14} - \Delta\text{H}_5 - 7\Delta\text{H}_8 + \Delta\text{H}_{21} + 6\Delta\text{H}_{15\alpha} + \Delta\text{H}_{18} - \Delta\text{H}_{19} - 7\Delta\text{H}_{22}$

<sup>a</sup> Mean.

<sup>b</sup> Two standard deviations of the mean.

<sup>c</sup> Number of measurements.

<sup>d</sup> Selected in this work, see text.

<sup>e</sup> Robie and Hemingway (1995).

<sup>f</sup> Lemire et al. (2020).

<sup>g</sup> Grevel and Majzlan (2011).

dissolved rapidly and reproducibly. The measured enthalpies of dissolution are summarized in Table 9. This table also shows the thermochemical cycles used to calculate the formation enthalpies of the metal tellurites and the formation enthalpies of the reference phases used in the calculations. The calculated formation enthalpies for the metal tellurites are listed in Table 10.

There are two specific properties of tellurium that need to be mentioned in connection with the validity of the calorimetric experiments. The first one is related to redox-active elements, including tellurium. The redox state of Te in the calorimetric solvent was not measured but assumed to be Te(IV) in each experiment. This assumption is based on numerous reports that the oxidation of Te(IV) to Te(VI) is extremely sluggish (Filella et al., 2019 and references therein). These authors wrote that ‘the older analytical literature abounds with complaints that the reduction may only be achieved by extremely strong reductants’, attesting to the inertness of Te(IV) towards oxidation or reduction. Therefore, parasitic heat effects related to redox reactions of Te(IV) cannot be expected in our calorimetric experiments.

The second property of tellurium is its volatilization in some aqueous media. Chen et al. (2016) concluded that Te is lost from 3 M HCl solutions at temperatures of 110 °C. They also found that the loss was not substantial, even at higher temperatures (200 °C). They speculated that the loss is driven by Te isotope fractionation between the liquid and gas phase. In our experiments, conducted at 25 °C, we see no evidence of prolonged parasitic reactions indicating loss of material from the solvent. Thus, for practical purposes, such loss can be neglected but could be of worry if the temperature of the calorimetric solvent should be increased.

### 3.9. Relaxation calorimetry

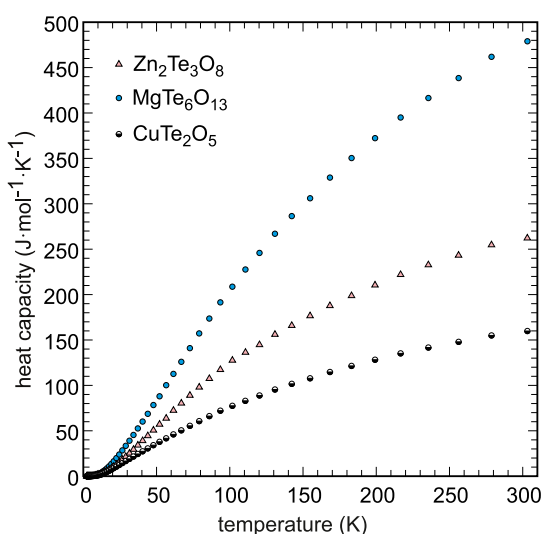
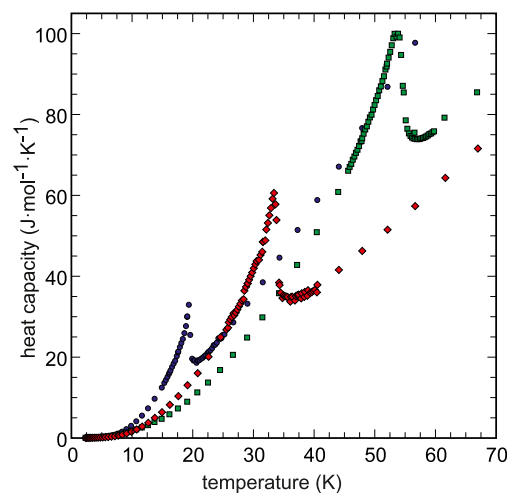
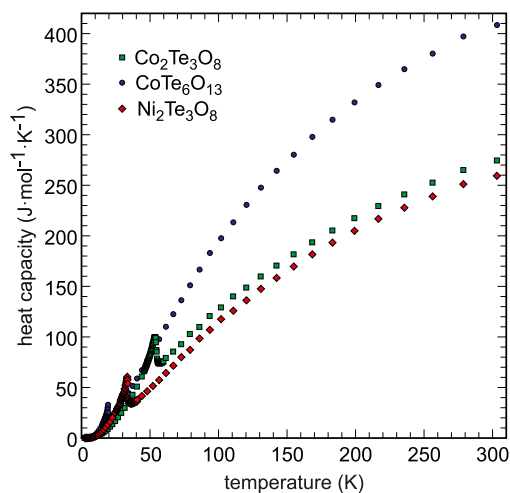
For a suite of selected samples, low-temperature (2–300 K) heat capacity ( $C_p$ ) was measured. Entropy at  $T = 298.15$  K was calculated by integration of the  $C_p/T$  functions (Table 10), where  $C_p$  was smoothed by several polynomials. The measured  $C_p$  data are available in electronic supplementary data files attached to this publication. For the phases  $\text{Zn}_2\text{Te}_3\text{O}_8$ ,  $\text{MgTe}_6\text{O}_{13}$ , and  $\text{CuTe}_2\text{O}_5$ , the  $C_p$  showed no anomalies over the temperature range of the measurements (Fig. 2).

For the phases  $\text{Co}_2\text{Te}_3\text{O}_8$ ,  $\text{CoTe}_6\text{O}_{13}$ , and  $\text{Ni}_2\text{Te}_3\text{O}_8$ , the  $C_p$  curves show lambda-shaped anomalies related to the magnetic transitions caused by the presence of Co or Ni (Fig. 3). The crests of the transitions are found at  $T = 54$  K for  $\text{Co}_2\text{Te}_3\text{O}_8$ ,  $T = 19.4$  K for  $\text{CoTe}_6\text{O}_{13}$ , and  $T = 33.4$  K for  $\text{Ni}_2\text{Te}_3\text{O}_8$ .

**Table 10**

Summary of thermodynamic data for the metal tellurites studied in this work, with comparison to previously published data. Data in parentheses were estimated.

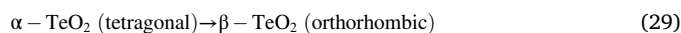
	$\Delta_f H^\circ$ kJ·mol <sup>-1</sup>	$S^\circ$ J·mol <sup>-1</sup> ·K <sup>-1</sup>	$\Delta_f S^\circ$ J·mol <sup>-1</sup> ·K <sup>-1</sup> This work	$\Delta_f G^\circ$ kJ·mol <sup>-1</sup>	$\Delta_f H^\circ$ kJ·mol <sup>-1</sup> Gospodinov and Bodganov (1984)
Co <sub>2</sub> Te <sub>3</sub> O <sub>8</sub>	-1514.2 ±6.0	319.2 ±2.2	-710.6 ±2.5	-1302.4 ±6.1	
CoTe <sub>6</sub> O <sub>13</sub>	-2212.5 ±8.1	471.7 ±3.3	-1190.1 ±3.5	-1857.7 ±8.2	
MgTe <sub>6</sub> O <sub>13</sub>	-2525.8 ±7.9	509.2 ±3.6	-1155.2 ±3.8	-2181.4 ±8.0	
Ni <sub>2</sub> Te <sub>3</sub> O <sub>8</sub>		293.3 ±2.1	-736.2 ±2.1		
NiTe <sub>6</sub> O <sub>13</sub>	-2198.7 ±8.2	(466.5) ±2.3	-1195.1 ±2.6	-1842.4 ±8.2	
CuTe <sub>2</sub> O <sub>5</sub>	-820.2 ±3.3	187.2 ±1.3	-458.2 ±1.4	-683.6 ±3.3	-662.5
Zn <sub>2</sub> Te <sub>3</sub> O <sub>8</sub>	-1722.5 ±4.0	299.3 ±2.1	-753.7 ±2.2	-1497.8 ±4.1	-1732.5

**Fig. 2.** Measured heat capacity for the phases Zn<sub>2</sub>Te<sub>3</sub>O<sub>8</sub>, MgTe<sub>6</sub>O<sub>13</sub>, and CuTe<sub>2</sub>O<sub>5</sub>.**Fig. 3.** Measured heat capacity for the phases Co<sub>2</sub>Te<sub>3</sub>O<sub>8</sub>, CoTe<sub>6</sub>O<sub>13</sub>, and Ni<sub>2</sub>Te<sub>3</sub>O<sub>8</sub>. Left: The entire data sets; right: detail showing the lambda-shaped C<sub>p</sub> anomalies at low temperatures.

## 4. Discussion

### 4.1. Thermodynamics of TeO<sub>2</sub>

In this work, we have specifically addressed the energetic difference between tetragonal and orthorhombic modifications of TeO<sub>2</sub>. The dissolution enthalpies for both polymorphs are listed in Table 9. From these enthalpies, the enthalpy of transformation for



can be calculated. The  $\Delta_r H_{29} = +1.40 \pm 0.07$  kJ·mol<sup>-1</sup>. The two polymorphs would be perfectly balanced in terms of their Gibbs free energies if  $\Delta_r G_{29} = 0 = \Delta_r H_{29} - T\Delta_r S_{29}$ . This condition would be satisfied if  $\Delta_r S_{29} = 4.7$  J·mol<sup>-1</sup>·K<sup>-1</sup>.

Entropies of polymorphs are similar but not equal. The entropies of the metastable polymorphs tend to be slightly higher than those of the stable polymorphs. For example, the entropies of cristobalite and tridymite are 4.5 and 5.8 % higher than that of quartz (Robie and Hemingway, 1995). The entropy of  $\gamma$ -Fe<sub>2</sub>O<sub>3</sub> is 6 % higher than that of hematite and the entropy of lepidocrocite 9 % higher than that of goethite (Majzlan et al., 2003). For the entropy of tellurite of 70.4 J·mol<sup>-1</sup>·K<sup>-1</sup> (Robie and Hemingway, 1995), an increase of 6 % amounts to 4.2 J·mol<sup>-1</sup>·K<sup>-1</sup>.

Therefore, the tetragonal polymorph is likely to be marginally stable with respect to the orthorhombic one. The difference is small and the reaction direction could be easily modified by particle-size effects

**Table 11**

Overview of published values of formation enthalpy for TeO<sub>2</sub>. All values in kJ·mol<sup>-1</sup>.

Thomsen (1882)	-322.9	Calorimetry
Mixter (1910)	-364.4	Calorimetry
Cordfunke et al. (1987)	-320.7 ± 3.2	Calorimetry
	-318.7 ± 7.4	Calorimetry
Abramchuk et al. (2020)	-320.4 ± 2.9	Calorimetry
Schneider and Zintl (1961)	-321.7 ± 5.0	Combustion calorimetry
Gadzhiev and Sharifov (1962)	-379.1 ± 1.3	Combustion calorimetry
Schuhmann (1925)	-325.5 <sup>a</sup>	EMF
Chatterji and Smith (1973)	-301.25	EMF
Mallika and Sreedharan (1986)	-321.1 ± 1.3	EMF
Aspiala et al. (2013)	-313.0 ± 1.8	EMF
Muenow et al. (1969)	-351.9 ± 12.0	High-T mass spectrometry
Robie and Hemingway (1995)	-319.7 ± 3.0	Evaluation
Wagman et al. (1982)	-322.6	Evaluation
Kubaschewski and Alcock (1979)	-323.4	Evaluation
Glushko et al. (1966)	-321.0	Evaluation
Coughlin (1954)	-325.1	Evaluation
Rossini et al. (1952)	-325.1	Evaluation

<sup>a</sup> Value corrected by Gehlen and Gehlen-Keller (1940).

(Majzlan, 2020) or impurities. We also note that at Moctezuma, a site exceptionally rich in Te, tellurite (β-TeO<sub>2</sub>) was reported to be more common than paratellurite (α-TeO<sub>2</sub>) (Gaines, 1970). This observation should be, however, confirmed by modern mineralogical techniques on bulk material before too much weight is assigned to it.

The TeO<sub>2</sub> glass is, as expected, metastable with respect to both crystalline polymorphs. The enthalpy of the reaction



is  $\Delta_f H_{30} = +14.09 \pm 0.11$  kJ·mol<sup>-1</sup>. The energetic difference between the crystalline tetragonal polymorph and the glass is substantial. The γ-TeO<sub>2</sub> phase, not measured in this work, is a product of devitrification of the TeO<sub>2</sub> glass and unstable with respect to α- and β-TeO<sub>2</sub>. Therefore, its enthalpy must lie between those of the glass and the orthorhombic polymorph.

The experimentally determined enthalpies of formation for TeO<sub>2</sub> scatter significantly (Table 11). Before briefly discussing the details, we have to note that most of the studies did not report which modification of TeO<sub>2</sub> was investigated. We assume, though, that it was the stable, tetragonal polymorph that was studied. A little of the scatter could be possibly assigned to the use of the orthorhombic instead of the tetragonal polymorph.

The two newer calorimetric studies of Cordfunke et al. (1987) and Abramchuk et al. (2020) converge to similar  $\Delta_f H^\circ$  values. Both studies used elemental Te as the reference compound. Cordfunke et al. (1987) dissolved Te and TeO<sub>2</sub> in acidic and alkaline aqueous solutions, Abramchuk et al. (2020) in molten sodium molybdate. The use of elemental Te as the reference compound and the excellent agreement of the derived  $\Delta_f H^\circ$  values may constitute a hint to their accuracy. These two values agree with the early datum of Thomsen (1882) who chlorinated Te to TeCl<sub>4</sub> and converted it in an aqueous solution to TeO<sub>2</sub>. Mixter (1910), on the other hand, obtained a much different  $\Delta_f H^\circ$  number. He oxidized both Te and TeO<sub>2</sub> to Te(VI) by reaction with sodium peroxide. It could be only speculated that the sluggish oxidation of aqueous Te species (Filella et al., 2019) led to irreproducible final states and introduced a systematic error in those measurements.

Combustion calorimetry of Schneider and Zintl (1961) gave a value very similar to those generated by most of the calorimetric studies. They very carefully analyzed the combustion products for elemental Te and for Te(VI); they also determined that the product was tetragonal TeO<sub>2</sub>. The results of the EMF measurements are scattered. Significant deviations are most likely explained by the need to extrapolate from high temperatures down to  $T = 298.15$  K. The value closest to our selected  $\Delta_f H^\circ$  below was obtained by Schuhmann (1925) who performed experiments at 25 and 45 °C. A similar value was derived by Mallika and

Sreedharan (1986) even though their experiments were running at elevated temperatures.

For the purposes of the processing of our calorimetric data, we selected an average of the values that cluster in the range of -318 to -326 kJ·mol<sup>-1</sup>. This average is  $-322.0 \pm 1.3$  kJ·mol<sup>-1</sup> and is used for the calculation of enthalpies of formation of the tellurites studied. We also note that all critical evaluations (see bottom portion of Table 11) selected a value from this range, suggesting that the  $\Delta_f H^\circ$  selected here is an accurate representation of the formation enthalpy of α-TeO<sub>2</sub> (tetragonal). Using this value and the dissolution enthalpies in Table 9, the formation enthalpy of β-TeO<sub>2</sub> (orthorhombic) is then  $-320.6 \pm 1.3$  kJ·mol<sup>-1</sup>.

#### 4.2. Metal tellurites

There are a few studies devoted to thermodynamics properties of tellurites. Heat capacity measurements were presented for Zn<sub>2</sub>Te<sub>3</sub>O<sub>8</sub> (Gospodinov and Atanasova, 2005), MnTe<sub>2</sub>O<sub>5</sub>, Mn<sub>2</sub>Te<sub>3</sub>O<sub>8</sub> (Gospodinov and Mihov, 1993), MnTe<sub>6</sub>O<sub>13</sub> (Gospodinov and Atanasova, 2006), MgTe<sub>2</sub>O<sub>5</sub>, Mg<sub>2</sub>Te<sub>3</sub>O<sub>8</sub>, MgTe<sub>6</sub>O<sub>13</sub> (Gospodinov, 1994a) and CuTe<sub>2</sub>O<sub>5</sub> (Gospodinov, 1994b). Enthalpies of formation of CuTe<sub>2</sub>O<sub>5</sub> and Zn<sub>2</sub>Te<sub>3</sub>O<sub>8</sub> were measured by reaction calorimetry by Gospodinov and Bogdanov (1984). Gibbs free energies of formation were determined for Ni<sub>2</sub>Te<sub>3</sub>O<sub>8</sub> and NiTe<sub>2</sub>O<sub>5</sub> by TeO<sub>2</sub>-vapor pressure measurements under high temperatures by Krishnan et al. (1999).

This work was specifically aimed at the anhydrous tellurites of Co, Cu, Mg, Mn, Ni, and Zn. Two important groups of tellurites were omitted because of experimental limitations. One of them are tellurites of iron. Preliminary syntheses showed that when not working in an inert atmosphere, the products are always too complex to extract a sample for calorimetry. In addition, many of the natural iron tellurites (e.g., emmonsite, Fe<sub>2</sub>(TeO<sub>3</sub>)<sub>3</sub>·2H<sub>2</sub>O; sonoraite, Fe(TeO<sub>3</sub>)(OH)·H<sub>2</sub>O) are hydrated, thus questioning the applicability of the data for anhydrous salts for natural settings. The other group are hydrated tellurites. Rajite, for example, was measured in this work but chemically similar hydrated tellurites (e.g., teineite, CuTeO<sub>3</sub>·2H<sub>2</sub>O) are much more common. Because the thermodynamic data for the hydrated tellurites are largely missing, the results of geochemical modeling with the data presented in this work should not be overinterpreted. A more complete data set for the naturally occurring tellurites would be needed to arrive at reliable conclusions.

Table 10 compares the data obtained previously to the values determined in this work. The agreement is fair for some phases (Zn<sub>2</sub>Te<sub>3</sub>O<sub>8</sub>) but very poor for other ones (CuTe<sub>2</sub>O<sub>5</sub>). The work of Gospodinov and Bogdanov (1984) was done as reaction calorimetry in a differential scanning apparatus. The products were not checked for their purity, thus possibly introducing large systematic errors.

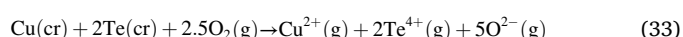
The large difference between the two values reported for CuTe<sub>2</sub>O<sub>5</sub> are a reason to critically scrutinize these results. The enthalpy of formation can be roughly estimated by a procedure outlined by Yoder and Flora (2005). They proposed that the lattice energies ( $U_L$ ) are roughly equal to the lattice energies of the simple components. For CuTe<sub>2</sub>O<sub>5</sub>,

$$U_L(\text{CuTe}_2\text{O}_5) = U_L(\text{CuO}) + 2U_L(\text{TeO}_2) \quad (31)$$

Yoder and Flora (2005) reported  $U_L(\text{CuO})$  as 4050 kJ·mol<sup>-1</sup>. They did not list  $U_L(\text{TeO}_2)$  but it can be calculated for the reaction.



as 11,194 kJ·mol<sup>-1</sup>, using enthalpy of formation for Te<sup>4+</sup>(g) from Wagman et al. (1982; 9196 kJ·mol<sup>-1</sup>), for O<sup>2-</sup> from Yoder and Flora (2005; 838 kJ·mol<sup>-1</sup>), and for α-TeO<sub>2</sub> from this work. Using Eq. (31),  $U_L(\text{CuTe}_2\text{O}_5) = 26,437$  kJ·mol<sup>-1</sup>. The enthalpy of the reaction



is  $\Delta H_{33} = 25,636$  kJ·mol<sup>-1</sup>, using the enthalpy of formation of

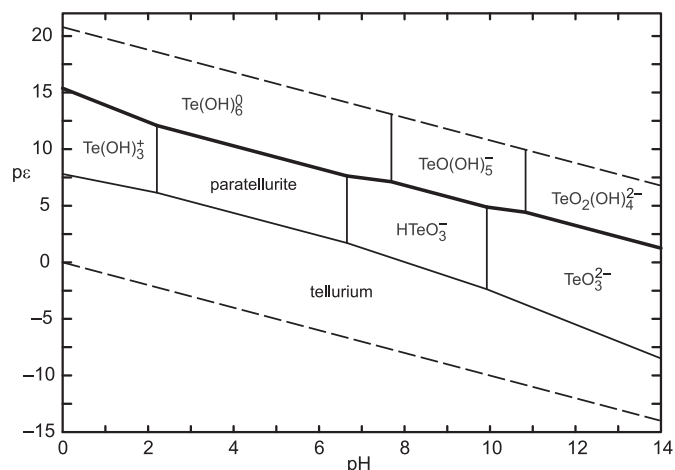


**Fig. 4.** pH-pe diagram for the system Te-O-H, with  $\log a(\text{Te}) = -4.5$ . If  $\log a(\text{Te})$  is lowered to  $-5$ , the field of paratellurite will disappear from the diagram and only aqueous species will appear for Te(IV) and Te(VI). The dashed lines show the boundaries of stability of water. The thick lines show the redox boundary of predominance of Te(IV) and Te(VI) species.

$\text{Cu}^{2+}(\text{g})$  from Wagman et al. (1982;  $3054 \text{ kJ}\cdot\text{mol}^{-1}$ ). The difference  $\Delta H_{33} - U_1(\text{CuTe}_2\text{O}_5)$  is the approximation of the formation enthalpy of  $\text{CuTe}_2\text{O}_5$  and is  $-801 \text{ kJ}\cdot\text{mol}^{-1}$ . This value compares favorably to the experimentally determined  $\Delta_f H^\circ(\text{CuTe}_2\text{O}_5)$  of  $-820.2 \pm 3.3$  in this work, the difference being 2.3 %, well within the error of the estimation method of Yoder and Flora (2005). On the other hand, it is 21 % off the value reported by Gospodinov and Bogdanov (1984), much more than the largest difference reported by Yoder and Flora (2005). These data give us confidence that the  $\Delta_f H^\circ(\text{CuTe}_2\text{O}_5)$  presented in this work is more accurate than that of Gospodinov and Bogdanov (1984).

#### 4.3. Environmental implications

Tellurium is a mineralogically diverse element (Christy, 2015) and the number of secondary Te minerals is impressive (Missen et al., 2020). Yet, thermodynamic data exist for very few of these minerals, making it difficult to construct phase diagrams that could be used to differentiate environments where the Te minerals form (e.g., by pH or total Te concentration). Phase diagrams can be constructed, for example for the Te-O-H system (Fig. 4), using the equilibrium constants of Filella and May (2019). It shows that paratellurite can precipitate from mildly to strongly acidic solutions at activities near saturation. If Cu or Zn is added to this system, the metal tellurites partially displace the stability field of paratellurite. A firmer statement about the formation conditions of these minerals must await thermodynamic measurements of other, competing phases in these systems.

It is also clear that these minerals form in 'hot spots' with Te concentrations much higher than the geochemical background. The background Te concentrations in freshwater, measured only in a few studies, range from tenths to tens of  $\text{ng}\cdot\text{L}^{-1}$  (see Belzile and Chen, 2015; Filella et al., 2019). Precipitation of rajite ( $\text{CuTe}_2\text{O}_5$ ), on the other hand, requires  $\sim 2300 \text{ ng Te}\cdot\text{L}^{-1}$  in the solution (at  $T = 298.15 \text{ K}$ ,  $\text{pH} = 7$ ,  $\log a(\text{Cu}^{2+}) = -3$ ). Under similar conditions ( $T = 298.15 \text{ K}$ ,  $\text{pH} = 7$ ,  $\log a(\text{Zn}^{2+}) = -3$ ), precipitation of zincspiroffite requires  $\sim 6100 \text{ ng Te}\cdot\text{L}^{-1}$  in the solution. These values are 3–5 orders of magnitude more than the natural background, not forgetting that the activities of  $\text{Cu}^{2+}$  and  $\text{Zn}^{2+}$  taken in these examples are fairly high. Under lower activities of such metals, encountered in unpolluted water, the amount of Te needed to supersaturate that water with respect to the studied metal tellurites would be much higher.

That certainly does not mean that solutions supersaturated with respect to the metal tellurites are found in large volumes. Our field

experience shows that many secondary minerals precipitate from a thin, essentially invisible film of aqueous solution and appear macroscopically dry whenever observed. In such way, very little volumes of the solutions need to become supersaturated to precipitate the Te(IV) phases. Such small volumes, or chemical microenvironments, were indeed described at Moctezuma (Mexico), a site exceptionally rich in Te and its minerals (Missen et al., 2022). These authors also investigated the response of living organisms to evaluated aqueous Te(IV) or Te(VI) concentrations. Tellurium appears to be toxic to the organisms which use different strategies to get rid of it: volatilization, precipitation of tellurium nanoparticles, or adsorption onto iron oxides (Missen et al., 2022). The phases studied here certainly do not control the solubility of Te in rivers and lakes. Instead, the available Te is probably dissolved, dispersed, adsorbed onto surfaces, or uptaken by biota, and these solutions are always undersaturated with respect to  $\text{TeO}_2$  or metal tellurites.

#### Declaration of competing interest

The authors declare that they have no known competing financial interests or personal relationships that could have appeared to influence the work reported in this paper.

#### Acknowledgements

We are thankful to three anonymous reviewers for their critical comments and especially one of them for thoughtful insights in Born-Haber cycle.

#### CRediT authorship contribution statement

JM: Conceptualization, acid-solution calorimetry, data reduction and interpretation, funding acquisition, writing; SN: syntheses of tellurites; PH: acid-solution calorimetry; EK, NT: synthesis of  $\text{TeO}_2$  glass; ED: relaxation calorimetry.

#### References

- Abramchuk, M., Lilova, K., Subramani, T., Yoo, R., Navrotsky, A., 2020. Development of high-temperature oxide melt solution calorimetry for p-block element containing materials. *J. Mater. Res.* 35, 2239.
- Agarwal, R., Singh, Z., 2006. Enthalpy increments of  $\text{Ba}_2\text{Te}_3\text{O}_8(\text{s})$  and  $\text{Ba}_3\text{Te}_2\text{O}_9(\text{s})$  compounds. *J. Alloys Compd.* 414, 230–234.
- Aspiala, M., Sukhomlinov, D., Taskinen, P., 2013. Standard Gibbs energy of formation of tellurium dioxide measurement by a solid-oxide electrolyte EMF technique. *Thermochim. Acta* 573, 95–100.
- Belzile, N., Chen, Y.-W., 2015. Tellurium in the environment: a critical review focused on natural waters, soils, sediments and airborne particles. *Appl. Geochem.* 63, 83–92.
- Beyer, H., 1967. Verfeinerung der Kristallstruktur von Tellurit, dem rhombischen  $\text{TeO}_2$ . *Z. Kristallogr.* 124, 228–237.
- Blanchandin, S., Marchet, P., Thomas, P., Champarnaud-Mesjard, J.C., Frit, B., Chagraoui, A., 1999. New investigations within the  $\text{TeO}_2$ - $\text{WO}_3$  system: phase equilibrium diagram and glass crystallization. *J. Mater. Sci.* 34, 4285–4292.
- Champarnaud-Mesjard, J.C., Thomas, P., Colas-Duttreilh, M., Oufkir, A., 2001. Crystal structure of dilead tritellurate (IV),  $\text{Pb}_2\text{Te}_3\text{O}_8$ . *Z. Kristallogr.* 216, 185–186.
- Chatterji, D., Smith, J.V., 1973. Free energy of formation of  $\text{Bi}_2\text{O}_3$ ,  $\text{Sb}_2\text{O}_3$ , and  $\text{TeO}_2$  from EMF measurements. *J. Electrochem. Soc.* 120, 889–893.
- Chen, Y.W., Alzahrani, A., Deng, T.L., Belzile, N., 2016. Valence properties of tellurium in different chemical systems and its determination in refractory environmental samples using hydride generation-atomic fluorescence spectroscopy. *Anal. Chim. Acta* 905, 42–50.
- Christy, A.G., 2015. Causes of anomalous mineralogical diversity in the periodic table. *Mineral. Mag.* 79, 33–49.
- Cooper, M.A., Hawthorne, F.C., 1996. The crystal structure of spiroffite. *Can. Mineral.* 34, 821–826.
- Cordfunke, E.H.P., Ouweltjes, W., Prins, G., 1987. Standard enthalpies of formation of tellurium compounds. I. Tellurium dioxide. *J. Chem. Thermodyn.* 19, 369–375.
- Coughlin, J.P., 1954. Contributions to the data on theoretical metallurgy. XII. Heats and free energies of formation of inorganic oxides. In: U. S. Bur. Mines Bull., 542.
- Elerman, Y., Koçak, M., 1986. Crystal data for  $\text{Sr}_2\text{Te}_3\text{O}_8$ . *J. Appl. Crystallogr.* 19, 410.
- Feger, C.R., Schimek, G.L., Kolis, J.W., 1999. Hydrothermal synthesis and characterization of  $M_2\text{Te}_3\text{O}_8$  ( $M = \text{Mn}, \text{Co}, \text{Ni}, \text{Cu}, \text{Zn}$ ): a series of compounds with the spiroffite structure. *J. Solid State Chem.* 143, 246–253.
- Filella, M., May, P.M., 2019. The aqueous chemistry of tellurium: critically-selected equilibrium constants for the low-molecular-weight inorganic species. *Environ. Chem.* 16, 289–295.

- Filella, M., Reimann, C., Biver, M., Rodushkin, I., Rodushkina, K., 2019. Tellurium in the environment: current knowledge and identification of gaps. *Environ. Chem.* 2019 (16), 215–228.
- Gadzhiev, S.N., Sharifov, K.A., 1962. The enthalpy of formation of  $\text{TeO}_2$ . *Izv. Akad. Nauk Azerb. Ser. Fiz. Mater.* 1, 47–53.
- Gaines, R.V., 1970. The Moctezuma tellurium deposit. *Mineral. Rec.* 1, 40–43.
- Gehlen, H., Gehlen-Keller, M., 1940. Zur Kenntnis der Thermodynamik des Telluridioxyds und seiner Umsetzung mit Schwefel. *Chem. Ber.* 73B, 1292–1298.
- Glushko, V.P., Medvedev, V.A., et al. (Eds.), 1966. *Termicheskie konstanty veshchestv. Part 2, 1966 (S, Se, Te, Po)*. Akademiya Nauk SSSR, Moscow.
- Gospodinov, G.G., 1994a. Heat capacities and derived thermodynamic properties of magnesium tellurates(IV). *J. Chem. Thermodyn.* 26, 143–146.
- Gospodinov, G.G., 1994b. Heat capacity of copper tellurates(IV) at temperatures from 350 K to 550 K. *J. Chem. Thermodyn.* 26, 1111–1113.
- Gospodinov, G., Atanasova, L., 2005. Heat capacities and thermodynamic functions of the tellurates(IV) of zinc and cadmium. *J. Thermal Anal. Calorim.* 82, 439–442.
- Gospodinov, G., Atanasova, L., 2006. Molar heat capacities of the tellurites  $\text{CoTeO}_3$ ,  $\text{MnTeO}_3$  and  $\text{MnTe}_6\text{O}_{13}$  in medium temperature range. *J. Thermal Anal. Calorim.* 83, 273–276.
- Gospodinov, G.G., Bogdanov, B.G., 1984. Determination of the heats of formation of some basic metal tellurites and pyrotellurites. *Thermochim. Acta* 81, 349–351.
- Gospodinov, G.G., Mihov, D.I., 1993. Molar heat capacities of the tellurites  $\text{MnTeO}_3$ ,  $\text{MnTe}_2\text{O}_5$ , and  $\text{Mn}_2\text{Te}_3\text{O}_8$ . *J. Chem. Thermodyn.* 25, 1249–1252.
- Grevel, K.-D., Majzlan, J., 2011. Thermodynamics of divalent metal sulfates. *Chem. Geol.* 286, 301–306.
- Hanke, K., Kupcik, V., Lindqvist, O., 1973. The crystal structure of  $\text{CuTe}_2\text{O}_5$ . *Acta Crystallogr.* 29, 963–970.
- Irvine, J.T.S., Johnston, M.G., Harrison, W.T.A., 2003. Lone-pair containment in closed cavities. The  $\text{MTe}_6\text{O}_{13}$  ( $M = \text{Mn, Ni, Co}$ ) family of ternary oxides. *J. Chem. Soc. Dalton Trans.* 3, 2641–2645.
- Johnston, M.G., Harrison, W.T.A., 2002. Manganese tellurite,  $\beta\text{-MnTe}_2\text{O}_5$ . *Acta Crystallogr. E* 58, 59–61.
- Kolar, D., Urbanc, V., Golic, L., Ravink, V., 1971. Thermal investigation of  $\text{NiTeO}_3$  and the synthesis of  $\text{Ni}_2\text{Te}_3\text{O}_8$ . *J. Inorg. Nuclear Chem.* 33, 3693–3697.
- Krishnan, K., Rao, G.A.R., Mudher, K.D.S., Venugopal, V., 1999. Vaporization behaviour and Gibbs energy of formation of  $\text{Ni}_2\text{Te}_3\text{O}_8$ ,  $\text{NiTe}_2\text{O}_5$  and  $\text{Ni}_3\text{TeO}_6$ . *J. Alloys Compd.* 288, 96–101.
- Kubaschewski, O., Alcock, C.B., 1979. *Tables of Metallurgical Thermochemistry*. van der Lee, A., Astier, R., 2007. Structural evolution in iron tellurates. *J. Solid-State Chem.* 180, 1243–1249.
- Lemire, R.J., Taylor, P., Palmer, D., Schlenz, H., 2020. *Chemical Thermodynamics: Chemical Thermodynamics of Iron, Part 2*. OECD Nuclear Energy Agency, 921 pp.
- Li, Y., Fan, W., Sun, H., Cheng, X., Li, P., Zhao, X., 2010. Structural, electronic, and optical properties of  $\alpha$ ,  $\beta$ , and  $\gamma\text{-TeO}_2$ . *J. Appl. Phys.* 107, 093506.
- Lieder, O.J., Gattow, G., 1969. Darstellung kristalliner Kobalt(II)-tellurite. *Naturwiss.* 56, 460.
- Lin, W.F., Xing, Q.J., Ma, J., Zou, J.P., Lei, S.L., Luo, X.B., Guo, G.C., 2013. Synthesis, band and crystal structures, and optical properties of the ternary compound  $\text{Mg}_2\text{Te}_3\text{O}_8$ . *Z. Anorg. Allg. Chem.* 639, 31–34.
- Majzlan, J., 2017. Solution calorimetry on minerals related to acid mine drainage – methodology, checks, and balances. *Acta Geol. Slov.* 9, 171–183.
- Majzlan, J., 2020. Processes of metastable-mineral formation in oxidation zones and mine wastes. *Mineral. Mag.* 84, 367–375.
- Majzlan, J., Lang, B.E., Stevens, R., Navrotsky, A., Woodfield, B.F., Boerio-Goates, J., 2003. Thermodynamics of iron oxides: part I. Standard entropy and heat capacity of goethite ( $\alpha\text{-FeOOH}$ ), lepidocrocite ( $\gamma\text{-FeOOH}$ ), and maghemite ( $\gamma\text{-Fe}_2\text{O}_3$ ). *Am. Miner.* 88, 846–854.
- Mallika, C., Sreedharan, O.M., 1986. Thermodynamic stabilities of  $\text{TeO}_2$  and  $\text{Sb}_2\text{Te}_3$  by a solid-oxide electrolyte e.m.f. technique. *J. Chem. Thermodyn.* 18, 727–734.
- Mandarino, J.A., Williams, S.J., Mitchell, R.S., 1963. Denningite, a new tellurite Mineral from Moctezuma, Sonora, Mexico. *Can. Mineral.* 7, 443–452.
- Mandarino, J.A., Williams, S.J., Mitchell, R.S., 1963. Spiroffite, a new tellurite mineral from Moctezuma, Sonora, Mexico. In: *Mineral. Soc. America, Special Paper*, 1, pp. 305–309.
- Miletich, R., 1993. Copper-substituted manganese-denningites,  $\text{Mn}(\text{Mn}_{1-x}\text{Cu}_x)(\text{Te}_2\text{O}_5)_2$  ( $0 \leq x \leq 1$ ): synthesis and crystal chemistry. *Miner. Petrol.* 48, 129–145.
- Missen, O.P., Ram, R., Mills, S.J., Etschmann, B., Reith, F., Shuster, J., Smith, D.J., Brugger, J., 2020. Love is in the earth: a review of tellurium (bio)geochemistry in surface environments. *Earth-Sci. Rev.* 204, 103150.
- Missen, O.P., Etschmann, B., Mills, S.J., Sanyal, S.K., Ram, R., et al., 2022. Tellurium biogeochemical transformation and cycling in a metalliferous semi-arid environment. *Geochim. Cosmochim. Acta* 321, 265–292.
- Mixter, W.G., 1910. Heat of formation of the oxides of molybdenum, selenium and tellurium; and fifth paper on the heat of combination of acidic oxides with sodium oxide. *Am. J. Sci. Ser. 4* (29), 488.
- Muenow, D.W., Hastle, J.W., Hauge, R., Bautista, R., Margrave, J.L., 1969. Vaporization, thermodynamics and structures of species in the tellurium + oxygen system. *Trans. Faraday Soc.* 65, 3210–3220.
- Nawash, J.M., Twamley, B., Lynn, K.G., 2007.  $\text{ZnTe}_6\text{O}_{13}$ , a new  $\text{ZnO-TeO}_2$  phase. *Acta Crystallogr. C* 63, 66–68.
- Petríček, V., Dušek, M., Palatinus, L., 2014. *Crystallographic Computing System Jana 2006: general features*. *Z. Kristallogr.—Cryst. Mater.* 229, 345–352.
- Platte, C., Trömel, M., 1981. Nickelditellurat(IV): Sauerstoffkoordinationszahl Fünf am vierwertigen Tellur. *Acta Crystallogr. B* 37, 1276–1278.
- Robie, R.A., Hemingway, B.S., 1995. Thermodynamic properties of minerals and related substances at 298.15 K and 1 bar ( $10^5$  Pascals) pressure and at higher temperatures. *U.S. Geol. Surv. Bull.* 2131, 461 p.
- Rossini, F.D., et al., 1952. Selected Values of Chemical Thermodynamic Properties, Natl. Bureau Stand., Circular 500.
- Schneider, A., Zintl, G.Z., 1961. Die Bildungsenthalpie des Telluridioxydes. *Anorg. Allg. Chem.* 308, 290–294.
- Schuhmann, R., 1925. The free energy and heat content of tellurium dioxide and of amorphous and metallic tellurium. The reduction potential of tellurium. *J. Am. Chem. Soc.* 47, 356–363.
- Shirkhanlou, M., Weil, M., 2013. The Mg member of the isotopic series  $\text{MTe}_6\text{O}_{13}$ . *Acta Crystallogr. F* 69, i18.
- Tagiara, N.S., Palles, D., Simandiras, E.D., Psycharis, V., Kyritsis, A., Kamitsos, E.I., 2017. Synthesis, thermal and structural properties of pure  $\text{TeO}_2$  glass and zinc-tellurite glasses. *J. Non-Cryst. Solids* 457, 116–125.
- Thomsen, J., 1882. In: *Thermochemische Untersuchungen, Band 2*. Barth, 405, p. 278.
- Trömel, M., Schmid, D., 1972. Tellurite des zweiwertigen Mangans, Kobalts und Nickels. *Z. Anorg. Allg. Chem.* 387, 230–240.
- Trömel, M., Ziethen-Reichnach, H., 1970. Magnesiumtellurite. *Z. Anorg. Allg. Chem.* 378, 238–244.
- Wagman, D.D., Evans, W.H., Parker, V.B., Schumm, R.H., Halow, I., Bailey, S.M., Churney, K.L., Nuttall, R.L., 1982. The NBS tables of chemical thermodynamic properties. Selected values for inorganic and C1 and C2 organic substances in SI units. *J. Phys. Chem. Ref. Data* 11 (supplement 2).
- Weil, M., 2017. Redetermination of the  $\gamma$ -form of tellurium dioxide. *IUCrData* 2, x171757.
- Weil, M., 2019.  $\text{Ca}_2\text{Te}_3\text{O}_8$ , a new phase in the  $\text{CaO-TeO}_2$  system. *Acta Crystallogr. E* 75, 26–29.
- Williams, S.A., 1979. Rajite, naturally occurring cupric pyrotellurite, a new mineral. *Mineral. Mag.* 43, 91–92.
- Wyckoff, R.W.G., 1963. *Crystal structures - volume 1*. In: *Structures*, Second edition 1. Interscience Publishers, New York Crystal, pp. 239–444.
- Yoder, C.H., Flora, N.J., 2005. Geochemical applications of the simple salt approximation to the lattice energies of complex materials. *Am. Mineral.* 90, 488–496. <https://doi.org/10.2138/am.2005.1537>.
- Zhang, P.H., Zhu, J.C., Zhao, Z.H., Gu, X.P., Lin, J.F., 2004. Zincospiroffite, a new tellurite mineral species from the Zhongshangou gold deposit, Hebei Province, People's Republic of China. *Can. Mineral.* 42, 763–768.